Article

Enantioselective Synthesis of Chiral Amines via Biocatalytic Carbene N—H Insertion

Viktoria Steck, DANIELA MARIA CARMINATI, Nathan Johnson, and Rudi Fasan

ACS Catal., **Just Accepted Manuscript** • DOI: 10.1021/acscatal.0c02794 • Publication Date (Web): 31 Aug 2020

Enantioselective Synthesis of Chiral Amines via Biocatalytic Carbene N—H Insertion

Viktoria Steck, Daniela M. Carminati, Nathan R. Johnson, and Rudi Fasan*

Department of Chemistry, University of Rochester, 14627 Rochester, New York, USA

* *Correspondence should be addressed to R.F. (rfasan@ur.rochester.edu)*

Abstract

Optically active amines represent highly valuable building blocks for the synthesis of advanced pharmaceutical intermediates, drug molecules, and biologically active natural products. Hemoproteins have recently emerged as promising biocatalysts for the formation of C—N bonds via carbene transfer, but asymmetric N—H carbene insertion reactions using these or other enzymes have so far been elusive. Here, we report the successful development of a biocatalytic strategy for the asymmetric N—H carbene insertion of aromatic amines with 2-diazopropanoate esters using engineered variants of myoglobin. High activity and stereoinduction in this reaction could be achieved by tuning the chiral environment around the heme cofactor in the metalloprotein in combination with catalyst-matching and tailoring of the diazo reagent. Using this approach, an efficient biocatalytic protocol for the synthesis of a broad range of substituted aryl amines with up to 82% *ee* was obtained. In addition, a stereocomplementary catalyst useful to access the mirror-image form of the N—H insertion products was identified. This work paves the way to asymmetric amine synthesis via biocatalytic carbene transfer, and the present strategy based on the synergistic combination of protein and diazo reagent engineering is expected to prove useful in the context of these as well as other challenging asymmetric carbene transfer reactions.

KEYWORDS: myoglobin, carbene transfer, asymmetric N—H insertion, chiral amines, protein engineering

Introduction

The asymmetric synthesis of chiral amines represents a highly sought-after goal in organic chemistry due to the ubiquitous presence of nitrogen containing functional groups in biologically active compounds.[1, 2] Nearly half of currently approved pharmaceuticals indeed comprise optically active amines. Prominent biocatalytic strategies for the enantioselective synthesis of chiral amines rely on the use of naturally occurring enzyme classes such as amine dehydrogenases, transaminases, ammonia lyases, aminomutases, and imine reductases.[3-8] More recently, engineered 'nitrene transferases' for asymmetric amine synthesis via C—H amination have also been developed.[9-11] In this context, the transition-metal catalyzed insertion of carbenoids into N—H bond represents an attractive and complementary strategy for forging new carbon-nitrogen bonds.[12-15] Hemoproteins have recently emerged as promising biocatalysts for promoting a variety of abiological carbene transfer reactions,[16-28] including N—H carbene insertions.[29, 30] In particular, we and the Arnold group have previously demonstrated that engineered variants of sperm whale myoglobin (Mb) and cytochrome $P450_{BM3}$, respectively, can catalyze carbene N—H insertion reactions involving aromatic amines and ethyl α-diazoacetate (EDA).[29, 30] More recently, the substrate scope of the myoglobin-based biocatalysts was extended toward the functionalization of benzylic and aliphatic amines.[31] In addition, artificial metalloenzymes have been also reported to be able to promote this reaction.[32-34] Despite this progress, biocatalytic strategies for asymmetric carbene N—H insertion have thus far remained elusive. The challenges inherent to realizing this transformation are further highlighted by studies focused on the development of organometallic catalysts for asymmetric N—H carbene insertions.[14, 15, 35, 36] The difficulty in achieving high activity and enantioselectivity in these reactions have been attributed to catalyst poisoning by the nucleophilic amine and facile dissociation of the ylide intermediate from the metal center, respectively.[14, 36] While significant progress was made toward overcoming these challenges, these chemocatalytic protocols require the use of precious metals (e.g., Rh, Pd),[37-40] synthetically challenging chiral ligands and/or co-catalysts,[37, 41-43] and/or are restricted to α-aryl diazo compounds,[39, 40, 44] with only a few exceptions.[42, 43] In this context, the development of biocatalytic alternatives would be therefore highly desirable as it will contribute to the development of sustainable and environmentally benign approaches for realizing these transformations. Herein, we report the development of an asymmetric strategy for the preparation of chiral amines via the myoglobin-catalyzed N—H insertion of aromatic amines with α-diazopropanoate esters. High activity and stereoinduction in this reaction could be achieved by tuning of the chiral environment around the heme cofactor in the metalloprotein in combination with catalyst-matching and tailoring of the diazo reagent. This work provides a new biocatalytic strategy for the synthesis of optically active α-amino acids and it demonstrates the value of a dual protein/substrate engineering approach for realizing challenging asymmetric carbene transfer reactions using an enzyme.

Results and Discussion

Target reaction and activity enhancement via diazo reagent optimization. The insertion of α-diazopropanoate esters into the N—H bond of aniline (**1**) was chosen as the target reaction. This reaction provides an attractive approach to the synthesis of chiral α-amino acids[45] as well as the preparation of chiral α-methyl-amine motifs occurring in various drug candidates.[46, 47] Using ethyl 2-diazopropanoate (EDP, **2a**) as the carbene donor, we initially tested the performance of myoglobin variant Mb(H64V,V68A), which was previously identified as an excellent biocatalyst for catalyzing the N—H insertion of ethyl 2-diazoacetate (EDA) with aniline and other arylamines.[29] In stark contrast to the reaction with EDA (6,150 turnovers or TON),[29] Mb(H64V,V68A) was found to exhibit a drastically reduced catalytic activity in the functionalization of aniline (**1**) with EDP (**2a**) to give the N—H insertion product **2b** (130 TON; **Figure 1**, Entry 2) under identical reaction conditions. The strikingly diminished activity of the hemoprotein in the reaction with EDP vs. EDA can be attributed to an increase in steric congestion at the level of the iron-carbenoid intermediate[48, 49] and/or a reduction of the electrophilicity due to the presence of the methyl group (vs. -H) in alpha to the carbene atom, resulting in overall reduced reactivity toward attack by the amine nucleophile. A similar trend was indeed observed in the context of Mb-catalyzed S—H insertion.[18]

To overcome this limitation, we decided to test the N—H insertion reactivity of Mb(H64V,V68A) in the presence of other 2-diazopropanoate esters such as isopropyl (**3a**), *tert*-butyl (**4a**), and benzyl derivatives (**5a**). While low TON values were observed for the reactions with **3a** and **4a** (13-27 TON), Mb(H64V,V68A) exhibited a significantly increased catalytic efficiency (835 TON) in the presence of benzyl 2-diazopropanoate (BnDP, **5a**) to give the N—H insertion product **5b**. Interestingly, a similar trend was observed using wild-type Mb as the catalyst.

Encouraged by these results, we examined a broader panel of myoglobin variants previously found to be active toward N—H insertion with EDA[29] in the aniline reaction with the differently substituted α-diazopropanoates **2a-5a**. As shown in **Figure 1**, all of these other myoglobin variants showed significantly higher catalytic turnovers in the N—H insertion reaction with benzyl 2-diazopropanoate **5a** (2,650 - 4,830 TON) compared to the corresponding reactions in the presence of the other diazopropanoate esters **2a-4a** (13 - 1,360 TON). Among them, Mb(H64V), Mb(L29A,H64V), and Mb(F43V,V68F) emerged as the most promising biocatalysts for the desired reaction, supporting 4,430 - 4,830 TON for conversion of aniline to **5b** in the presence of BnDP (**5a**). The beneficial effect of the benzyl substituent in the diazo substrate was apparent also for other Mb variants such as Mb(F43V) and Mb(V68A), which exhibited 4,090 and 3,095 TON, respectively, toward the synthesis of **5b** as opposed to their negligible activity toward formation of **2b-4b**.

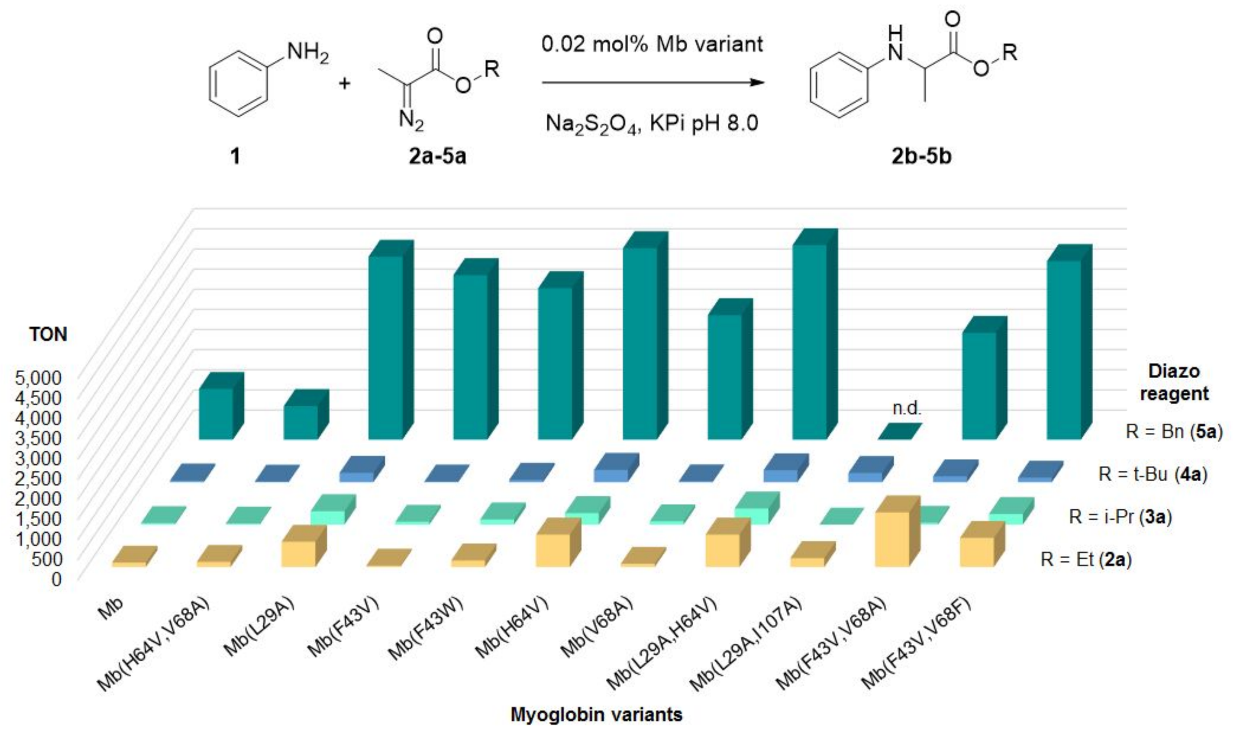

Figure 1. Catalytic activity (TON) of wild-type Mb, Mb(H64V,V68A), and other engineered Mb variants toward the N—H insertion of aniline with the 2-diazopropanoate esters **2a-5a**. Reaction conditions: 10 mM aniline **1**, 10 mM **2a-5a**, 1 μM Mb catalyst, 10 mM $Na_2S_2O_4$, 50 mM phosphate buffer (pH 8). See **Table S1** for further details.

Optimization of enantioselectivity via protein engineering. Having identified BnDP (**5a**) as a well-matched carbene donor reagent for achieving high activity in the desired N—H insertion reaction with an α-diazopropanoate substrate, we assessed the enantioselectivity of the aforementioned Mb-catalyzed transformations (**Table 1**). Despite their high catalytic activity, none of these Mb variants was found to induce significant levels of enantiomeric excess (*ee*) in the N—H insertion reaction (2 - 4% *ee*, **Table 1**, Entries 1 and 14; Supporting Information **Table S2**). Disappointingly, further mutagenesis of Mb(L29A,H64V), which was one of the most active biocatalysts identified from the initial screening (**Figure 1**), did not yield variants with improved enantioselectivity (Supporting Information, **Table S2**). Based on these results, we decided to screen a broader collection of Mb-based 'carbene transferases', which were previously developed for various asymmetric carbene transfer reactions,[17-20, 24, 25, 28] including asymmetric S—H insertion reactions.[18] Despite differing by multiple mutations at the level of their 'active site' residues (L29, F43, H64, V68, and I107), none of these metalloproteins show noticeable levels of enantioselectivity toward the N—H insertion reaction with aniline (**1**) and **5a** (-3 - 4% *ee*, Supporting Information, **Table S2**). These results underscored the fundamental challenges of achieving high enantioselectivity in an asymmetric carbene N—H insertions as anticipated at the incipit of this work.

Pursuing an alternative approach toward this goal, we turned our attention to modification of the highly conserved[50] proximal heme-coordinating histidine residue (His93; **Figure S1**) in the Mb(H64V,V68A) background. Accordingly, we tested the performance in the N—H insertion reaction of a series of Mb(H64V,V68A)-based variants in which the His93 residue is substituted for both metal-coordinating (i.e., Cys, Asp, Ser, Tyr) and non-nucleophilic residues (i.e. Phe, Ala). Gratifyingly, these experiments revealed a pronounced effect of the axial ligand substitution on the enantioselectivity of the N—H insertion reaction, especially in the presence of Ser, Ala, or Tyr in place of His93 (**Table 1**, Entries 2-7). From these analyses, Mb(H64V,V68A,H93Y) was identified as the most enantioselective catalyst for this reaction, producing **5b** with an enantiomeric excess of 20% while maintaining good activity (1,180 TON). We also tested the effect of introducing non-canonical amino acids such as *N*-methyl histidine (NMH), β-(3-thienyl)-alanine (3ThA), (3-(3'-pyridyl)-alanine (3PyA) and *p*-aminophenylalanine (pAmF) at the His93 position of Mb(H64V,V68A) (**Table 1**, Entries 9-11). While these axial ligand modifications have produced functional carbene transferases,[51] none of these mutations had a beneficial impact on the enantioselectivity of the present reaction.

From these studies, we selected Mb(H64V,V68A,H93Y) as the most promising candidate for further optimization of its enantioselectivity via protein engineering. To facilitate these efforts, we established that these Mb-catalyzed transformations can be carried out using *E. coli* whole cells expressing the Mb(H64V,V68A,H93Y) biocatalyst. Interestingly, the whole-cell reactions brought about a slight improvement in enantioselectivity compared to the *in vitro* reactions with purified protein (20→28% *ee*; **Table 1,** Entries 1 vs. 8). Using this approach, Mb(H64V,V68A,H93Y) was subjected to site-saturation mutagenesis at the active site positions corresponding to Leu29 and Phe43, followed by screening of the resulting variants as whole cells arrayed in multi-well plates. While the large majority of these quadrupole mutants showed reduced enantioselectivity compared to the parent enzyme (see **Table S2** for representative examples), an improved variant carrying a Leu29Met substitution could be identified. Mb(L29M,H64V,V68A,H93Y) catalyzes the formation of **5b** with an improved enantioselectivity of 53% *ee* compared to 28% ee for Mb(H64V,V68A,H93Y) (**Table 1**, Entries 12 vs. 8; see also **Figure 2**). Furthermore, the Leu29Met mutation was found to be beneficial also toward increasing the efficiency of the reaction, resulting in an improved yield of 94% compared to 39% for the parent enzyme. Site-saturation mutagenesis of the yet unaltered active site position 107 in Mb(L29M,H64V,V68A,H93Y) failed to give further improvements in enantioselectivity. Combined with the results from the screening efforts mentioned earlier, these protein engineering studies revealed both a strong cooperativity of the active site mutations in dictating and controlling protein-induced stereoinduction and a highly rugged fitness landscape[52] with respect to this property. Indeed, while resulting in folded and functional variants, other substitutions at position 29 (e.g., L29H, L29K) and both isosteric (e.g., F43H) and non-isosteric (e.g., F43C, F43I) substitutions at position 43 were found to lead to nearly complete loss of stereoselectivity (1-14% *ee*; Supporting Information **Table S3**, Entries 2-9). At position 107, only β-branched residues structurally related to the wild-type isoleucine residue (i.e., Thr and Val) were tolerated without a complete loss of enantioselectivity (38-42% ee vs. 53% ee; Supporting Information **Table S3**, Entries 10 and 11).

Table 1. Catalytic activity and enantioselectivity of selected engineered myoglobin variants in the N—H insertion reaction with aniline **1** and benzyl 2-diazopropanoate **5a**.[a]

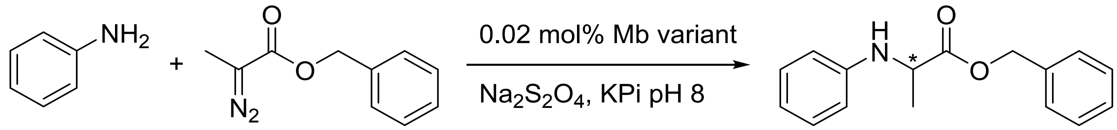

Entry	Catalyst	Yield[b]	TON[b]	% *ee*[c]
1	Mb(H64V,V68A)	41%	2,030	2
2	Mb(H64V,V68A,H93A)	20%	980	16
3	Mb(H64V,V68A,H93C)	19%	960	8
4	Mb(H64V,V68A,H93D)	21%	1,040	2
5	Mb(H64V,V68A,H93F)	14%	700	1
6	Mb(H64V,V68A,H93S)	15%	750	13
7	Mb(H64V,V68A,H93Y)	24%	1,180	20
8	Mb(H64V,V68A,H93Y)[e]	39%	-	28
9	Mb(H64V,V68A,H93(NMH))	6%	310	6
10	Mb(H64V,V68A,H93(3ThA))	24%	1,195	4
11	Mb(H64V,V68A,H93(3PyA))	17%	830	-6
12	Mb(H64V,V68A,H93(pAmF))	26%	1,300	3
13	Mb(L29M,H64V,V68A,H93Y)[e]	94%	-	53
14	Mb(F43V,V68F)	40%	1,990	4
15	Mb(F43V,H64A,V68F)	39%	1,960	-43
16	Mb(F43V,H64A,V68F)[e]	64%	-	-56
17	Mb(F43V,H64C,V68F)[e]	36%	-	42
18	Mb(F43V,H64G,V68F)	34%	1,700	-17
19	Mb(F43V,H64T,V68F)[e]	33%	-	48

[a]Reaction conditions: 5 mM **1**, 5 mM **5a**, 1 μM Mb catalyst, 50 mM phosphate buffer (pH 8), room temperature. [b]Yield and TON determined based on HPLC conversion using calibration curves with isolated **5b**. [c]Enantiomeric excess determined by chiral SFC. [e]Reaction conditions: 5 mM **1**, 5 mM **5a**, *E. coli* whole cells expressing Mb catalyst (OD=20), 50 mM phosphate buffer (pH 7.2), room temperature.

Based on these results, we decided to explore an alternative evolutionary trajectory starting from Mb(F43V,V68F), which was one of the most active biocatalysts for the N—H insertion reaction with BnDP as identified from the screening of the initial panel of Mb variants (>5,000 TON, **Figure 1**). In this case, site-saturation mutagenesis was directed to the distal His64 residue, as mutation of this position was also determined to be beneficial to improve catalytic activity in this reaction (i.e., Mb(H64A), **Figure 1**). Screening of this library enabled the identification of two variants, Mb(F43V,H64C,V68F) and Mb(F43V,H64T,V68F), featuring improved enantioselectivity (4% → 42% and 48% *ee*, respectively) for the synthesis of the same enantiomer of **5b** generated using Mb(L29M,H64V,V68A,H93Y) (**Figure 2**). The latter remained a superior biocatalyst for this transformation, however, in reasons of its slightly higher enantioselectivity and better yield (93% vs. 33-36%). Interestingly, two Mb variants with inverted enantioselectivity were also identified from this Mb(F43V,V68F)-based library, bearing a His64→Gly or His64→Ala mutation (**Table 1**, Entries 18 and 15). Mb(F43V,H64A,V68F), in particular, was determined to be the most promising biocatalyst for achieving enantiocomplementarity in this reaction, enabling the synthesis of **5b** in -56% *ee* and 64% yield using whole-cells and with identical enantiopreference and -43% *ee* using purified protein (**Table 1**, Entries 16 vs. 15; see also **Figure 2**). Further mutagenesis of position 29 and 107 in Mb(F43V,H64A,V68F) did not yield further improvements in enantioselectivity (see **Table S3** for selected examples). As noted earlier for Mb(L29M,H64V,V68A,H93Y), a strong synergy among the active site mutations in influencing enantioselectivity became apparent also for the stereocomplementary counterpart Mb(F43V,H64A,V68F), as judged by the low enantioselectivity (0-4% *ee*) of both Mb(F43V,V68F) and the single-site variant Mb(H64A) (Supporting Information, **Table S2**). In addition, the high sensitivity of this property to subtle modifications of Mb active site configuration was evident from the complete switch in enantiopreference (48% ee vs. -56% *ee*) observed for Mb(F43V,H64T,V68F) vs. Mb(F43V,H64A,V68F), which is induced by a small change at position 64 (Thr vs. Ala).

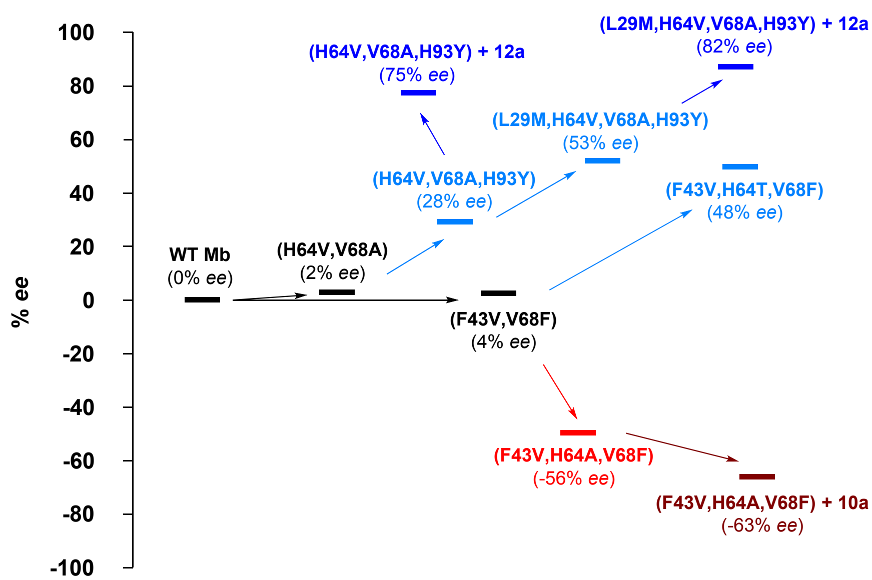

Figure 2. Optimization of enantioselectivity of Mb-catalyzed N—H insertion reaction with aniline and α-diazopropanoate esters via protein and substrate engineering. When not specified, the diazo reagent is BnDP (**5a**).

Optimization of enantioselectivity via tailoring of the diazo substrate. From the studies summarized above, Mb(L29M,H64V,V68A,H93Y) and Mb(F43V,H64A,V68F) emerged as the most selective biocatalysts for the synthesis of **5b** with complementary enantioselectivity (**Figure 2**). Given our results with the different diazopropanoate esters (**Figure 1**), we envisioned that modification of the carbene donor reagent could offer an additional strategy, complementary to protein engineering, to further fine-tune the enantioselectivity of these Mb-catalyzed transformations. Specifically, we surmised that modification of the benzyl group in BnDP, which was critical for imparting high activity in this reaction (**Figure 1**), could provide a means to influence also stereoinduction, possibly through affecting the facial selectivity of amine attack to the heme-bound carbenoid and/or via other mechanisms. Accordingly, we investigated the reactivity of Mb(L29M,H64V,V68A,H93Y) toward the aniline functionalization reaction in the presence of a panel of benzyl 2-diazopropanoate derivatives in which a methyl substituent was added in *ortho*- (**6a**), *meta*- (**7a**), and *para*- (**8a**) position of the aromatic ring of the benzyl group (**Figure 3**). Gratifyingly, these experiments revealed a major effect of the methyl substitution pattern on the enantioselectivity of the reaction, with the use of 4-methylbenzyl 2-diazopropanoate **8a** enabling the largest increase in enantiomeric excess of the corresponding N—H insertion product **9b** compared to the reaction in the presence of **5a** (53→68% *ee*). In comparison, the reactions with **7a** and **6a** resulted in a more modest improvement (62% *ee*) and a reduction (25% *ee*), respectively, of enantioinduction under identical experimental conditions, revealing a correlation between this property and the increasing distance of the steric bulk derived from the methyl group (i.e., *para* > *meta* > *ortho*) from the α-carbon atom of the diazo reagent, and thus of the heme-carbenoid intermediate.[48] Based on these findings, we tested the *para*-trifluoromethyl- and *para*-methoxy-substituted diazo reagents **9a** and **10a**, respectively, which led to the formation of the corresponding products **9b** and **10b** in comparable enantiomeric excess (67% *ee*) as observed for the *para*-methyl-substituted counterpart **8b** (**Figure 3**). These results indicated that substrate-dependent steric effects are primarily responsible for affecting the enzyme's enantioselectivity compared to electronic factors. Based on that and given the higher enantioselectivity levels obtained for **8b** and **7b** over **6b**, we chose to further increase the steric bulk in the *para* and *meta* position of the aryl ring in the diazo compound by using the 3,4-dimethyl- (**11a**), 4-isopropyl (**12a**) and 4-*tert*-butyl (**13a**) substituted diazo reagents. Gratifyingly, these modifications resulted in a further improvement of enantioselectivity, with the best results being obtained with **12a** to give the N—H insertion product **12b** in 82% *ee* and 51% yield (**Figure 3**). Beside their beneficial effect on stereoselectivity, it is worth noting that all of the diazopropanoate reagents were readily accepted by Mb(L29M,H64V,V68A,H93Y) without a significant drop in the yield of these reactions (50-87% vs. 93%; **Figure 3**), thus denoting a good tolerance of the biocatalyst also in the presence of relatively bulky reagents such as **13b**. To examine the generality of this substrate engineering approach, we also tested the panel of 2-diazopropanoate esters in the presence of Mb(H64V,V68A,H93Y) as the catalyst. Insightfully, a very similar structure-enantioselectivity trend was obtained for this biocatalyst (i.e., 4-^{i}Pr ≈ 4-^{t}Bu ≥ 4-CF_3 > 4-MeO ≈ 3,4-dimethyl = 4-Me >> 3-Me >> 2-Me; **Scheme S1**) compared to that observed for Mb(L29M,H64V,V68A,H93Y) (i.e., 4-^{i}Pr > 4-^{t}Bu > 3,4-dimethyl ≥ 4-CF_3= 4-Me = 4-MeO > 3-Me >> 2-Me). Furthermore, an even larger improvement in enantioselectivity was observed in the case of the former enzyme (i.e., 28%→75% *ee* vs. 53→82% *ee*) upon re-engineering of the diazo reagent (**Scheme S1**).

Similar experiments were then conducted using the enantio-complementary biocatalyst Mb(F43V,H64A,V68F). Also in this case, substitution of the benzyl group was found to affect the enantioselectivity of the biocatalyst (**Figure 3**), further supporting the generality of this strategy. At the same time, an overall different structure-activity profile was obtained for this Mb variant compared to Mb(L29M,H64V,V68A,H93Y) and Mb(H64V,V68A,H93Y), which is not surprising since the benzyl group in the corresponding heme-carbenoid intermediates is expected to interact with different regions of the active site in the two enantiodivergent catalysts. For Mb(F43V,H64A,V68F), most of the other *para* substitutions were tolerated without significant change in the performance of the biocatalyst, whereas both a 2-methyl (**6b**) and 4-^{t}Bu substitution in the diazo compound (**13b**) reduced enantioselectivity (-30% *ee* and -37% *ee*) compared to the reaction with BnDP (-56% *ee*). In contrast, an improvement in both enantioselectivity (-56% → -63% *ee*) and yield (64%→ 94%) was achieved using the 4-methoxy substituted diazopropanoate derivative **10a**, resulting in the formation of **10b** in -63% *ee* and 94% yield. Importantly, for all of the Mb variants tested, the performance of these biocatalysts could be further optimized via re-engineering of the diazo compound, demonstrating the value of this strategy as a complement to protein engineering.

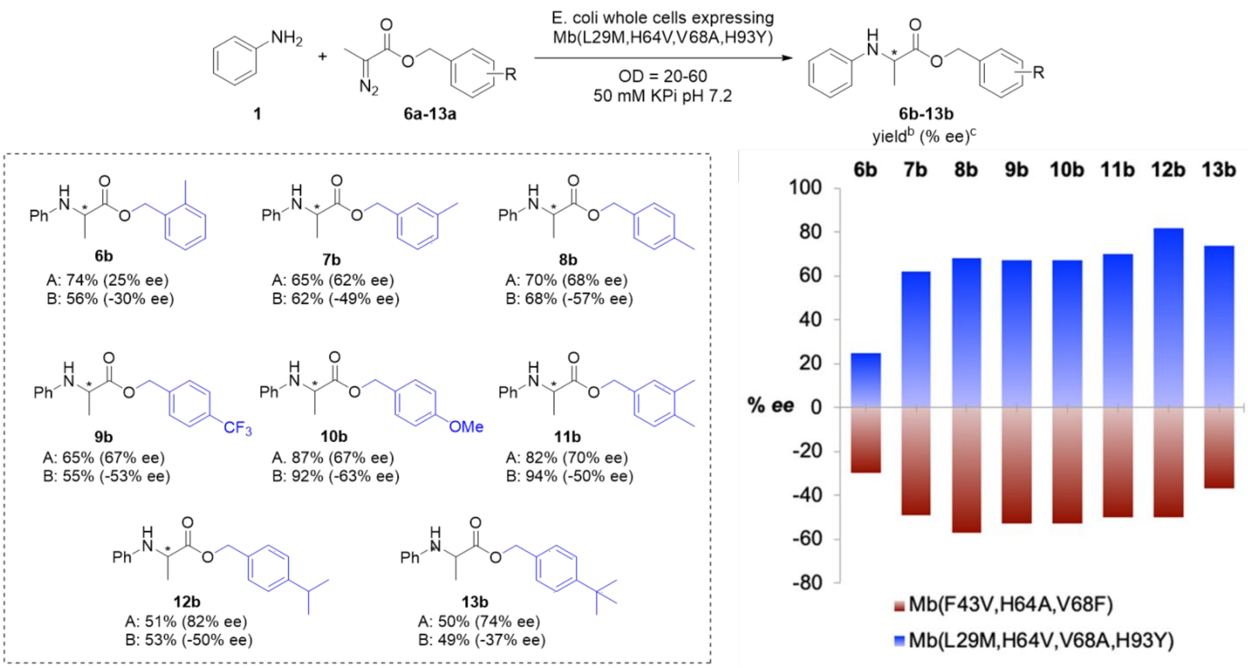

Figure 3. Substrate scope (left box) and comparison of enantioselectivity (right graph) for Mb(L29M,H64V,V68A,H93Y) (*blue*) and Mb(F43V,H64A,-V68F) (*orange*) in the N—H insertion reaction with aniline **1** and substituted benzyl 2-diazopropanoates **6a-13a**. Reaction conditions: 5 mM aniline, 5 mM **6a-13a**, *E. coli* whole cells expressing Mb catalyst (OD=20), 50 mM phosphate buffer (pH 7.2), room temperature. [b] Yield determined based on HPLC conversion using calibration curves with isolated **6b-13b**. [c] Enantiomeric excess determined by chiral SFC.

Optimization of the Mb(L29M,H64V,V68A,H93Y)-catalyzed reaction. Having identified **12a** as the best matched carbene donor reagent for the Mb(L29M,H64V,V68A,H93Y)-catalyzed N—H insertion reaction, the latter was subjected to further optimization and characterization (**Table 2**). Using a 1:2 aniline:diazo compound ratio, the yield of **12b** from the whole cell reaction with this enzyme could be increased from 51% to 82% while maintaining high enantioselectivity (79% *ee*; **Table 2**, Entry 3 vs. 1). Under these conditions, nearly quantitative yields (94-98%) for this reaction could be obtained using a higher cell density (OD_{600}) of 40-60 (vs. 20), albeit with a reduction in enantiopurity (74% *ee*; **Table 2**, Entry 5-6).

Table 2. Mb(L29M,H64V,V68A,H93Y)-catalyzed enantioselective N—H insertion reaction with aniline **1** and substituted benzyl 2-diazopropanoate (**6a-13a**) under different conditions.[a]

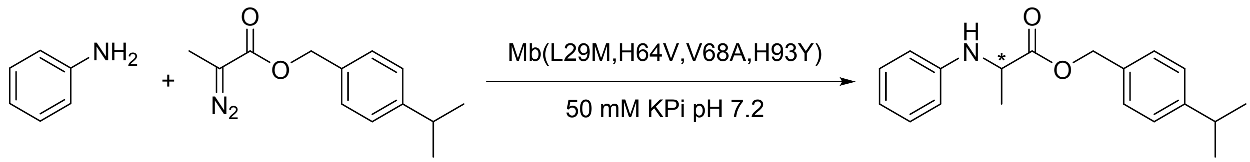

1 **12a** **12b**

Entry	Catalyst loading	Aniline (**1**)	Diazo (**12a**)	Yield[b]	TON[b]	% *ee*[c]
1	OD=20	5 mM	5 mM	51%	n.d.	82
2	OD=20	10 mM	5 mM	61%	151	80
3	OD=20	5 mM	10 mM	82%	202	79
4	OD=10	5 mM	10 mM	80%	509	70
5	OD=40	5 mM	10 mM	94%	119	74
6	OD=60	5 mM	10 mM	98%	79	74
7	20 μM	5 mM	10 mM	54%	137	36
8	5 μM	5 mM	10 mM	55%	571	30
9	1 μM	5 mM	10 mM	47%	2,470	28
10	5 μM	2.5 mM	10 mM	80%	399	30

[a] Reaction conditions: **1** and **12a** at the indicated concentration, Mb(L29M,H64V,V68A,H93Y) catalyst in whole cells or as purified protein at the indicated OD_{600} or concentration, respectively, in 50 mM phosphate buffer (pH 7.2), room temperature. [b] Yield and TON determined based on HPLC conversion using calibration curves with isolated **12b**. n.d. = not determined. [c] Enantiomeric excess determined by chiral SFC.

Further characterization of Mb(L29M,H64V,V68A,H93Y) in purified form showed that it supports up to 2,470 total turnovers for the formation of **12b** (**Table 2**, Entry 9), with an initial rate of 100 turnovers/min. The reaction reaches completion within 60 minutes.[29] Interestingly, both yield and enantioselectivity of the N—H insertion reactions with purified Mb(L29M,H64V,V68A,H93Y) were generally inferior than those obtained from the whole-cell reactions with cells expressing this Mb variant (**Table 2**, Entries 3-6 vs. 7-10), indicating a beneficial effect of the intracellular environment on the performance of the biocatalyst possibly due to macromolecular crowding or other factors. In addition, also Mb(H64V,V68A,H93Y) and Mb(F43V,H64A,V68F) exhibit this trend (**Table 1**, Entries 7 vs. 8, 15 vs. 16). This phenomenon has been observed before for enzymatic reactions,[53] including certain biocatalytic carbene transfer reactions.[54] We further noticed that a comparable yield of 50-60% was obtained in the presence of 5 mM aniline across variable catalyst loading conditions (i.e., between 0.02 and 0.4 mol%), whereas a higher yield could be achieved by reducing the substrate concentration (55% → 80%; **Table 2**, Entries 8 vs. 10). These results suggest the presence of product inhibition. Supporting this conclusion, controls experiment showed that a Mb(L29M,H64V,V68A,H93Y) reaction with

4-bromoaniline as the substrate (*vide infra*) gave the expected N—H insertion product in the absence but not in the presence of **12b** spiked into to the reaction mixture. Interestingly, no signs of product inhibition were observed for the whole-cell reaction, adding to the benefits of the latter approach for performing these transformations. Although the reasons for this phenomenon were not investigated, we hypothesize that it could derive from a favorable effect of macromolecular crowding toward destabilizing the product/enzyme complex and/or from efficient diffusion (or export) of the N—H insertion product outside of the cell, both of which are expected to relieve the biocatalyst from product inhibition effects.

Analysis of the Amine Substrate Scope. Using the reaction conditions optimized above, we next investigated the performance of Mb(L29M,H64V,V68A,H93Y) toward enabling the asymmetric insertion of diazopropanoate **12a** across different aromatic amines (**Scheme 1**). Notably, a broad range of aniline derivatives (**16a-i**) could be efficiently transformed by the enzyme to give the desired N—H insertion products in good to excellent yields (50-99%) and good enantioselectivity (57-81% *ee*). Specifically, Mb(L29M,H64V,V68A,H93Y) was found to tolerate well both electron-withdrawing (**16e-f**) and electron-donating (**16c-d**) substituents in the *para* position of the aniline substrate, exhibiting a generally higher enantioselectivity toward functionalization of the latter (70-81% vs. 57-60% *ee*, respectively). Similar results were obtained for *meta*-substituted aniline derivatives **16b** and **16g**which could be converted into **17b** and **17g** in 74-88% yield and 74-78% *ee*. The *ortho*-substituted aniline derivative **17a** was obtained in quantitative yield (99%) but with a lower enantioselectivity of 31% *ee*, indicating that *meta* and *para* substitution are better tolerated than *ortho* substitutions with respect to enantioselectivity as judged based on the **17a-c** regioisomer series. A sterically encumbered substrate such as 4-*tert*-butyl aniline (**16i**) was also accepted by the catalyst, although an increase in steric bulk at the *para* position affected both yield and enantioselectivity, as derived from comparison of the results with **16i** with those for the isopropyl- (**16h**) and methyl-substituted (**16c**) counterparts. 2-Naphthylamine was also tested but found not to participate in this reaction (data not shown), likely due to the poor solubility of this compound in the aqueous reaction media.

Scheme 1. Substrate scope of Mb(L29M,H64V,V68A,H93Y) (**A**) and Mb(F43V,H64A,V68F) (**B**) in the N—H insertion reaction with α-alkyl diazoesters and substituted anilines **16a-i**.[a]

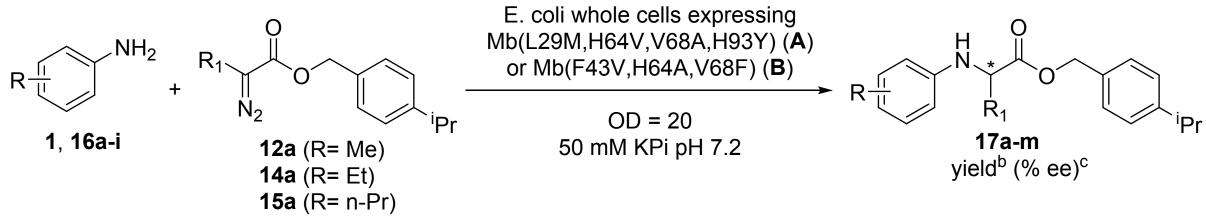

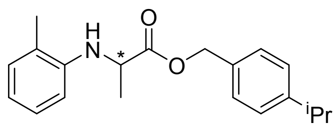
17a
A: 99% (31% ee)
B: 99% (-9% ee)

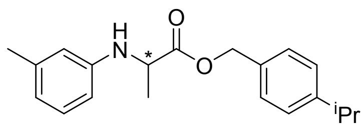
17b
A[d]: 88% (78% ee)
B: 62% (-53% ee)

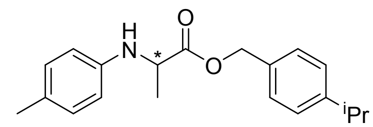
17c
A[d]: 75% (70% ee)
B: 49% (-64% ee)

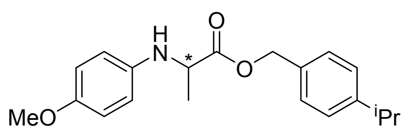
17d
A: 54% (81% ee)
B: 65% (-43% ee)

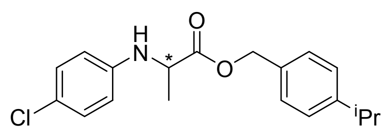
17e
A: 76% (60% ee)
B: 59% (-20% ee)

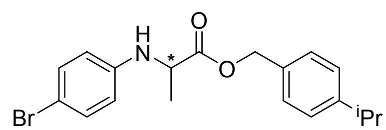
17f
A: 94% (57% ee)
B: 93% (-31% ee)

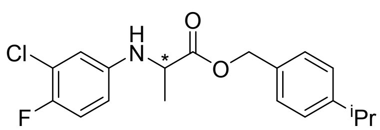
17g
A: 74% (74% ee)
B: 64% (-5% ee)

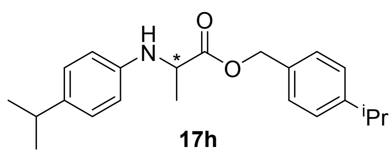
17h
A[d]: 74% (63% ee)
B: 56% (-40% ee)

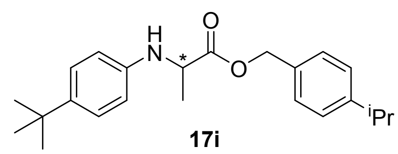
17i
A: 50% (44% ee)
B: 78% (-38% ee)

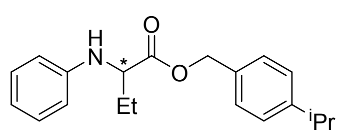
17k
A: 77% (8% ee)
B: 43% (-41% ee)

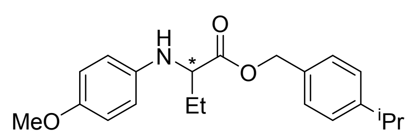
17j
A: 84% (22% ee)
B: 60% (-29% ee)

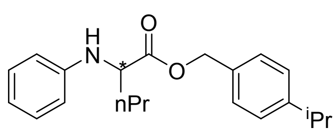
17l
A: 51% (15% ee)
B: 44% (-5% ee)

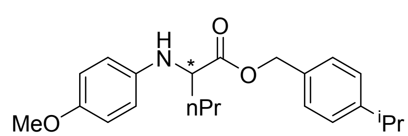
17m
A: 65% (13% ee)
B: 25% (-6% ee)

[a] Reaction conditions: 5 mM aniline, 10 mM **12a** or **14a** or **15a**, *E. coli* whole cells expressing Mb catalyst (OD=20), 50 mM phosphate buffer (pH 7.2), room temperature. [b] Yield determined based on HPLC conversion using calibration curves with isolated product. [c] Enantiomeric excess determined by chiral SFC. [d] Reaction performed using OD=60.

Having established the broad substrate scope of Mb(L29M,H64V,V68A,H93Y), we were interested in comparing and contrasting the performance of the enantiocomplementary catalyst Mb(F43V,H64A,V68F) across the same set of substrates (**Scheme 1**). In all cases, Mb(F43V,H64A,V68F) was able to process the aryl amine derivative, furnishing the corresponding N—H insertion product **17a-m** with a yield ranging from 49% to 99%. In addition, for all substrates, this biocatalyst furnished the opposite enantiomer with respect to Mb(L29M,H64V,V68A,H93Y), thus exhibiting a consistent enantiodivergent selectivity compared to the latter. While sharing with Mb(L29M,H64V,V68A,H93Y) a comparably broad substrate scope, Mb(F43V,H64A,V68F) was found to display a much more pronounced substrate-dependent effect on enantioselectivity, which varied from -5% to -64% *ee* (**Scheme 1**). The substituent effect on stereoselectivity also differed between the two biocatalysts. For example, while in both cases substitutions in *para* and *meta* of the aniline substrate are better tolerated than *ortho* substitutions (e.g., **17b** and **17c** vs. **17a**), the results with **17i**, **17h**, and **17c** indicate that the enantioselectivity of Mb(F43V,H64A,V68F) is significantly less affected by increasing steric bulk at the *para* position (Me > ^{i}Pr = ^{t}Bu) when compared with Mb(L29M,H64V,V68A,H93Y) (Me > ^{i}Pr > ^{t}Bu). Mb(F43V,H64A,V68F)-dependent stereoinduction is also significantly more sensitive to the electronic properties of the substituent (e.g., **17c** vs. **17e**). We attribute the differential behavior of two catalysts as emerging from these and the studies with the different diazopropanoate esters (**Figure 3**) to different mode of interaction with the diazo reagent and aniline substrate, and further studies are warranted to elucidate these aspects in more detail.

For both catalysts, we then tested their performance in the asymmetric N—H insertion with aniline (**1**) and a representative aniline derivative (i.e., p-methoxy-aniline, **16d**) in the presence of other α-alkyl substituted diazoesters, namely the α-diazobutanoate reagent **14a** and α-diazopentanoate **15a** (**Scheme 1**). Notably, both catalysts were able to readily accept these carbene donor reagents to give the desired products **17k-17m** in good to moderate yields (51-84% for (Mb(L29M,H64V,V68A,H93Y) and 25-60% for Mb(F43V,H64A,V68F; **Scheme 1**). In addition, the two biocatalysts maintained enantiodivergent selectivity in these reactions. Not surprisingly, however, the enantioselectivity of these reactions was significantly diminished compared to the reactions with the α-diazopropanoate reagent **12a** (see **12b** in **Figure 3** and **17d** in **Scheme 1**), supporting the importance of the diazo reagent/catalyst match for optimal chiral induction. As an exemption, the Mb(F43V,H64A,V68F) catalyst was found to tolerate a larger substituent (Et) at the alpha position of the diazo reagent, producing **17k** and **17j** with enantiomeric excess values comparable to those for the α-methyl substituted counterparts (-41% *ee* vs. -50% ee and -29% *ee* vs. -41% *ee*, respectively)**.**

Conclusions

In conclusion, we have reported the first example of a biocatalytic strategy for the asymmetric synthesis of chiral amines via carbene N—H insertion. Specifically, an engineered myoglobin catalyst capable of promoting the insertion of 2-diazopropanoates into the N—H bonds of a broad range of aniline derivatives with up to 99% yield and up to 82% *ee* was developed. In addition, a stereodivergent biocatalyst that offers up to -64% *ee* for the same reaction was obtained, thus providing access to both enantiomeric forms of the desired N—H insertion product. These reactions can be carried out in whole cell systems, which simplify their application for organic synthesis. Our protein engineering studies revealed a highly cooperative effect of beneficial active site mutations in inducing and controlling stereoselectivity in this reaction, but also highlighted the challenge of achieving high enantiocontrol through this strategy alone. As demonstrated by the present studies, tailoring and catalyst-matching of the diazo reagent provided an effective strategy for both enhancing the catalytic efficiency (**Figure 1**) and optimizing the enantioselectivity (**Figures 2** and **3**) of this metalloprotein-catalyzed reaction. To the best of our knowledge, this is the first example of the use of diazo substrate engineering for fine-tuning the stereoselectivity of an enzyme-catalyzed carbene transfer reaction. This work lays the foundation for future development of other asymmetric N—H insertions and it is anticipated that the present strategy based on the synergistic combination of protein and diazo reagent engineering could prove valuable toward developing biocatalytic strategies for these and other challenging asymmetric carbene-mediated transformations.

Experimental Details

Reagents and Analytical Methods. All chemicals and reagents were purchased from commercial suppliers (Sigma-Aldrich, TCI Chemicals) and used without any further purification, unless otherwise stated. The diazo compounds isopropyl 2-diazopropanoate (**3a**), *tert*-butyl 2-

diazopropanoate (**4a**) and benzyl 2-diazopropanoate (**5a**) were prepared according to previously reported procedures.[1] All moisture- or oxygen-sensitive reactions were carried out under argon atmosphere in oven-dried glassware with magnetic stirring using standard gas-tight syringes, cannulae and septa. ^{1}H, ^{19}F and ^{13}C NMR spectra were measured on a Bruker DPX-400 instrument (operating at 400 MHz for ^{1}H, 376 MHz for ^{19}F and 100 MHz for ^{13}C) or a Bruker DPX-500 instrument (operating at 500 MHz for ^{1}H and 125 MHz for ^{13}C). Tetramethylsilane (TMS) served as the internal standard (0 ppm) for ^{1}H NMR, $CDCl_3$ was used as the internal standard (77.0 ppm) for ^{13}C NMR. Silica gel chromatography purifications were carried out using AMD Silica Gel 60 Å 230-400 mesh. Thin Layer Chromatography (TLC) was carried out using Merck Millipore TLC silica gel 60 F254 glass plates. UV-Vis measurements were performed on a Shimadzu UV-2401PC UV-Vis spectrometer. HPLC analyses were performed on a Shimadzu LC-2010A-HT equipped with a VisionHT C18 column and a UV-Vis detector. Stereoisomer resolution was performed by Supercritical Fluid Chromatography (SFC) analysis, using a JASCO Analytical and Semi-Preparative SFC instrument.

Cloning and Mutagenesis. pET22b(+) (Novagen) was used as the recipient plasmid vector for cloning of all of the myoglobin variants. The plasmids encoding for the selected engineered variant of sperm whale myoglobin were prepared as described previously.[2] The Mb(H64V,V68A,H93Y) and Mb(F43V,H64A,V68F)-derived single-site saturation libraries were prepared by using "small intelligent mutagenesis"[3] as described previously.[4] Using the corresponding gene encoding the parent protein as template, small-intelligent mutagenesis libraries for each of the four target active site positions (i.e., 29, 43, 64, and 107) were prepared using a mixture of four primers containing the codon NDT, VMA, ATG and TGG at the target position in a 12 : 6 : 1 : 1 ratio. After gene assembly via SOE PCR, the corresponding library was cloned into the *Nde* I / *Xho* I cassette of pET22b(+), followed by transformation into *E. coli* DH5α cells. As an example, for preparing the site-saturation mutagenesis library at position 64, a 3'-terminal fragment of the target gene was prepared by PCR (NEB Phusion Polymerase) using a 12 : 6 : 1 : 1 mixture of forward primers #18 through #21, the reverse super primer #2, and vector pET22b_Mb(F43V,V68F) as template. In a separate PCR reaction, the 5'-terminal gene fragment was prepared using forward super primer #1, reverse primer #22, and vector pET22b_Mb(F43V,V68F) as template. The two fragments were then fused together using stitching with overlap extension PCR (SOE PCR) and super primers #1 and #2 to yield the target gene encoding for Mb(F43V,H64X,V68F) where X is the randomized position. The plasmid pET22b(+) and the SOE product were digested with *Nde* I and *Xho* I for 2 hr at 37 °C. The gene insert and plasmid were then ligated with T4 DNA ligase. The ligation mix was transformed into chemically competent *E. coli* DH5α cells. At least 60 colonies per library were pooled, sequenced, and transformed into chemically competent *E. coli* C41(DE3) cells for expression. The sequences of the oligonucleotide primers used in this project are given in **Table S4**.

Protein expression and purification. Wild-type Mb and engineered Mb variants were cloned and expressed in *E. coli* C41(DE3) cells as described previously.[2] Briefly, cells were grown in TB medium (ampicillin, 100 mg L^{-1}) at 37 °C (180 rpm) until OD_{600} reached 0.8-1.0. Cells were then induced with 0.25 mM β-D-1-thiogalactopyranoside (IPTG) and 0.3 mM δ-aminolevulinic acid (ALA). After induction, cultures were shaken at 27 °C (180 rpm), harvested after 20 h by centrifugation (4,000 rpm, 20 min, 4 °C) and resuspended in Ni-NTA Lysis Buffer (50 mM KPi, 250 mM NaCl, 10 mM histidine, pH 8.0). Resuspended cells were frozen and stored at -80 °C. Cell suspensions were thawed at room temperature, lysed by sonication, and clarified by centrifugation (14,000 rpm, 50 min, 4 °C). The clarified lysate was transferred to a Ni-NTA column equilibrated with Ni-NTA Lysis Buffer. The protein was washed with Ni-NTA Wash Buffer (50 mM KPi, 250 mM NaCl, 20 mM histidine, pH 8.0). Proteins were eluted with Ni-NTA Elution Buffer (50 mM KPi, 250 mM NaCl, 250 mM histidine, pH 7.0). After buffer exchange (50 mM Kpi, pH 7.0), the proteins were stored at +4 °C. Myoglobin concentration was determined by UV/Vis spectroscopy using an extinction coefficient of ε_{410} = 157 mM^{-1} cm^{-1}.

N—H insertion reactions. Under standard reaction conditions, reactions were carried out at a 400 μL scale using 1 or 20 μM myoglobin, 5 mM amine, 5 or 10 mM diazo compound, and 10 mM sodium dithionite. In a typical procedure, in an anaerobic chamber, a solution containing the desired myoglobin variant was mixed with a solution of sodium dithionite in argon purged potassium phosphate buffer (50 mM, pH 8.0). Reactions were initiated by addition of amine (400 mM stock solution in EtOH) followed by the addition of diazo compound (400 mM stock solution in EtOH), and the reaction mixtures were stirred in the chamber for 12 h at room temperature. For whole cell experiments, the cell suspensions stored at -80 °C were thawed at room temperature, centrifuged, resuspended in reaction buffer (potassium phosphate buffer (50 mM, pH 7.2) supplemented with micronutrients) and adjusted to the desired OD_{600}. Under standard reaction conditions, reactions were carried out at a 400 μL scale using *E. coli* whole cells expressing the desired myoglobin variant, 5 mM amine and 5 or 10 mM diazo compound. The cells were transferred to an anaerobic chamber, and reactions were initiated by addition of amine (400 mM stock solution in EtOH) followed by the addition of diazo compound (400 mM stock solution in EtOH), and the reaction mixtures were stirred in the chamber for 12 h at room temperature.

Product inhibition experiment. Reaction was carried out at a 400 μL scale using 5 μM myoglobin, 2.5 mM benzyl phenylalaninate (**5b**), 2.5 mM 4-bromoaniline, 10 mM diazo compound, and 10 mM sodium dithionite. In a typical reaction, a solution containing sodium dithionite (100 mM stock solution) in potassium phosphate buffer (50 mM, pH 7.2) was degassed by bubbling argon into the mixture for 3 min in a septum-capped vial. A buffered solution containing the myoglobin variant was carefully degassed in a similar manner in a separate vial. The two solutions were then mixed together via cannula. Benzyl phenylalaninate was then added (2.5 μL from a 0.4 M stock solution in EtOH) and the reaction was stirred at room temperature. After 15 min, 5 μL of 4-bromoaniline (from a 0.4 M stock solution in EtOH) and 10 μL of EDA (from a 0.4 M stock solution in DMF) were added with a syringe. The reaction was stirred for 16 hours at room temperature, under positive argon pressure.

Product analysis. The reactions were analyzed by adding 8 μL of internal standard (fluorenone, 50 mM in DMSO) to the reaction mixture, followed by extraction with 400 μL of dichloromethane. The organic layer was removed via evaporation and the residue was dissolved in 300 μL methanol, filtered through 0.22 μm syringe filters, and analyzed by SFC and HPLC (see the Supporting Information Reagents and Analytical Methods section for details on SFC and HPLC analyses). Calibration curves for quantification of the different N—H insertion products were constructed using authentic standards prepared as described in the Supporting Information Synthetic Procedures. All measurements were performed at least in duplicate. For each experiment, negative control samples containing either no enzyme or no reductant were included.

Synthetic Procedures and Product characterization. Detailed procedures and characterizations for the synthesis of aryl diazopropanoates (**6a-15a**), intermediates and N—H insertion products (**6b-13b**, **17a-17m**) are provided in the Supporting Information.

Associated Content

Supporting figures, oligonucleotide sequences, compound characterization data and NMR spectra. This material is available free of charge via the Internet at http://pubs.acs.org.

Acknowledgements

This work was supported by the U.S. National Institute of Health grant R01 GM098628. N.R.J. would like to thank RIT COS D-RIG for summer support. The authors are grateful to Kathryn Goerl for technical support. MS instrumentation at the University of Rochester was supported by the National Science Foundation grants CHE-0840410 and CHE-0946653.

References

(1) Ghislieri, D., and Turner, N. J. Biocatalytic Approaches to the Synthesis of Enantiomerically Pure Chiral Amines, *Top. Catal.* **2014**, *57*, 284-300.

(2) Breuer, M., Ditrich, K., Habicher, T., Hauer, B., Kesseler, M., Sturmer, R., and Zelinski, T. Industrial methods for the production of optically active intermediates, *Angew. Chem. Int. Ed.* **2004**, *43*, 788-824.

(3) Nestl, B. M., Hammer, S. C., Nebel, B. A., and Hauer, B. New Generation of Biocatalysts for Organic Synthesis, *Angew. Chem. Int. Ed.* **2014**, *53*, 3070-3095.

(4) Fuchs, M., Farnberger, J. E., and Kroutil, W. The Industrial Age of Biocatalytic Transamination, *Eur. J. Org. Chem.* **2015**, *2015*, 6965-6982.

(5) Parmeggiani, F., Weise, N. J., Ahmed, S. T., and Turner, N. J. Synthetic and Therapeutic Applications of Ammonia-lyases and Aminomutases, *Chem. Rev.* **2018**, *118*, 73-118.

(6) Mangas-Sanchez, J., France, S. P., Montgomery, S. L., Aleku, G. A., Man, H., Sharma, M., Ramsden, J. I., Grogan, G., and Turner, N. J. Imine reductases (IREDs), *Curr. Opin. Chem. Biol.* **2017**, *37*, 19-25.

(7) Kelly, S. A., Pohle, S., Wharry, S., Mix, S., Allen, C. C. R., Moody, T. S., and Gilmore, B. F. Application of omega-Transaminases in the Pharmaceutical Industry, *Chem. Rev.* **2018**, *118*, 349-367.

(8) Groger, H. Biocatalytic concepts for synthesizing amine bulk chemicals: recent approaches towards linear and cyclic aliphatic primary amines and -substituted derivatives thereof, *Appl. Microbiol. Biotechnol.* **2019**, *103*, 83-95.

(9) Singh, R., Bordeaux, M., and Fasan, R. P450-catalyzed intramolecular sp3 C—H amination with arylsulfonyl azide substrates, *ACS Catal.* **2014**, *4*, 546-552.

(10) Hyster, T. K., Farwell, C. C., Buller, A. R., McIntosh, J. A., and Arnold, F. H. Enzyme-Controlled Nitrogen-Atom Transfer Enables Regiodivergent C-H Amination, *J. Am. Chem. Soc.* **2014**, *136*, 15505-15508.

(11) Prier, C. K., Zhang, R. J. K., Buller, A. R., Brinkmann-Chen, S., and Arnold, F. H. Enantioselective, Intermolecular Benzylic C—H Amination Catalysed by an Engineered Iron-Haem Enzyme, *Nat. Chem.* **2017**, *9*, 629-634.

(12) Doyle, M. P., and Ye, T. (1998) *Modern catalytic methods for organic synthesis with diazo compounds*, Wiley, New York.

(13) Ford, A., Miel, H., Ring, A., Slattery, C. N., Maguire, A. R., and McKervey, M. A. Modern Organic Synthesis with alpha-Diazocarbonyl Compounds, *Chem. Rev.* **2015**, *115*, 9981-10080.

(14) Zhu, S. F., and Zhou, Q. L. Transition-metal-catalyzed enantioselective heteroatom-hydrogen bond insertion reactions, *Acc. Chem. Res.* **2012**, *45*, 1365-1377.

(15) Gillingham, D., and Fei, N. Catalytic X-H insertion reactions based on carbenoids, *Chem. Soc. Rev.* **2013**, *42*, 4918-4931.

(16) Coelho, P. S., Brustad, E. M., Kannan, A., and Arnold, F. H. Olefin Cyclopropanation via Carbene Transfer Catalyzed by Engineered Cytochrome P450 Enzymes, *Science* **2013**, *339*, 307-310.

(17) Bordeaux, M., Tyagi, V., and Fasan, R. Highly Diastereoselective and Enantioselective Olefin Cyclopropanation Using Engineered Myoglobin-Based Catalysts, *Angew. Chem. Int. Ed.* **2015**, *54*, 1744–1748.

(18) Tyagi, V., Bonn, R. B., and Fasan, R. Intermolecular carbene S-H insertion catalysed by engineered myoglobin-based catalysts, *Chem. Sci.* **2015**, *6*, 2488-2494.

(19) Tyagi, V., and Fasan, R. Myoglobin-Catalyzed Olefination of Aldehydes, *Angew. Chem. Int. Ed.* **2016**, *55*, 2512-2516

(20) Tyagi, V., Sreenilayam, G., Bajaj, P., Tinoco, A., and Fasan, R. Biocatalytic Synthesis of Allylic and Allenyl Sulfides through a Myoglobin-Catalyzed Doyle-Kirmse Reaction, *Angew. Chem. Int. Ed.* **2016**, *55*, 13562-13566.

(21) Kan, S. B. J., Lewis, R. D., Chen, K., and Arnold, F. H. Directed evolution of cytochrome c for carbon-silicon bond formation: Bringing silicon to life, *Science* **2016**, *354*, 1048-1051.

(22) Prier, C. K., Hyster, T. K., Farwell, C. C., Huang, A., and Arnold, F. H. Asymmetric Enzymatic Synthesis of Allylic Amines: A Sigmatropic Rearrangement Strategy, *Angew. Chem. Int. Ed.* **2016**, *55*, 4711-4715.

(23) Kan, S. B. J., Huang, X., Gumulya, Y., Chen, K., and Arnold, F. H. Genetically programmed chiral organoborane synthesis, *Nature* **2017**, *552*, 132-136.

(24) Chandgude, A. L., and Fasan, R. Highly Diastereo- and Enantioselective Synthesis of Nitrile-Substituted Cyclopropanes by Myoglobin-Mediated Carbene Transfer Catalysis, *Angew. Chem. Int. Ed.* **2018**, *57*, 15852-15856.

(25) Vargas, D. A., Tinoco, A., Tyagi, V., and Fasan, R. Myoglobin-Catalyzed C-H Functionalization of Unprotected Indoles, *Angew. Chem. Int. Ed.* **2018**, *57*, 9911-9915.

(26) Chen, K., Huang, X. Y., Kan, S. B. J., Zhang, R. K., and Arnold, F. H. Enzymatic construction of highly strained carbocycles, *Science* **2018**, *360*, 71-75.

(27) Zhang, R. K., Chen, K., Huang, X., Wohlschlager, L., Renata, H., and Arnold, F. H. Enzymatic assembly of carbon-carbon bonds via iron-catalysed sp(3) C-H functionalization, *Nature* **2019**, *565*, 67-72.

(28) Chandgude, A. L., Ren, X., and Fasan, R. Stereodivergent Intramolecular Cyclopropanation Enabled by Engineered Carbene Transferases, *J. Am. Chem. Soc.* **2019**, *141*, 9145-9150.

(29) Sreenilayam, G., and Fasan, R. Myoglobin-catalyzed intermolecular carbene N-H insertion with arylamine substrates, *Chem. Commun.* **2015**, *51*, 1532-1534.

(30) Wang, Z. J., Peck, N. E., Renata, H., and Arnold, F. H. Cytochrome P450-catalyzed insertion of carbenoids into N-H bonds, *Chem. Sci.* **2014**, *5*, 598-601.

(31) Steck, V., Sreenilayam, G., and Fasan, R. Selective Functionalization of Aliphatic Amines via Myoglobin-Catalyzed Carbene N-H Insertion, *Synlett* **2020**, *31*, 224-229.

(32) Sreenilayam, G., Moore, E. J., Steck, V., and Fasan, R. Metal substitution modulates the reactivity and extends the reaction scope of myoglobin carbene transfer catalysts, *Adv. Synth. Cat.* **2017**, *359*, 2076–2089.

(33) Wolf, M. W., Vargas, D. A., and Lehnert, N. Engineering of RuMb: Toward a Green Catalyst for Carbene Insertion Reactions, *Inorg. Chem.* **2017**, *56*, 5623-5635.

(34) Moore, E. J., Steck, V., Bajaj, P., and Fasan, R. Chemoselective Cyclopropanation over Carbene Y-H Insertion Catalyzed by an Engineered Carbene Transferase, *J. Org. Chem.* **2018**, *83*, 7480-7490.

(35) Moody, C. J. Enantioselective insertion of metal carbenes into N-H bonds: A potentially versatile route to chiral amine derivatives, *Angew. Chem. Int. Ed.* **2007**, *46*, 9148-9150.

(36) Ren, Y. Y., Zhu, S. F., and Zhou, Q. L. Chiral proton-transfer shuttle catalysts for carbene insertion reactions, *Org. Biomol. Chem.* **2018**, *16*, 3087-3094.

(37) Xu, B., Zhu, S. F., Xie, X. L., Shen, J. J., and Zhou, Q. L. Asymmetric N-H Insertion Reaction Cooperatively Catalyzed by Rhodium and Chiral Spiro Phosphoric Acids, *Angew. Chem. Int. Ed.* **2011**, *50*, 11483-11486.

(38) Zhu, Y., Liu, X. H., Dong, S. X., Zhou, Y. H., Li, W., Lin, L. L., and Feng, X. M. Asymmetric N-H Insertion of Secondary and Primary Anilines under the Catalysis of Palladium and Chiral Guanidine Derivatives, *Angew. Chem. Int. Ed.* **2014**, *53*, 1636-1640.

(39) Xu, B., Zhu, S. F., Zuo, X. D., Zhang, Z. C., and Zhou, Q. L. Enantioselective N-H insertion reaction of alpha-aryl alpha-diazoketones: an efficient route to chiral alpha-aminoketones, *Angew. Chem. Int. Ed.* **2014**, *53*, 3913-3916.

(40) Arredondo, V., Hiew, S. C., Gutman, E. S., Premachandra, I. D. U. A., and Van Vranken, D. L. Enantioselective Palladium-Catalyzed Carbene Insertion into the N-H Bonds of Aromatic Heterocycles, *Angew. Chem. Int. Ed.* **2017**, *56*, 4156-4159.

(41) Liu, B., Zhu, S. F., Zhang, W., Chen, C., and Zhou, Q. L. Highly enantioselective insertion of carbenoids into N-H bonds catalyzed by copper complexes of chiral spiro bisoxazolines, *J. Am. Chem. Soc.* **2007**, *129*, 5834-5835.

(42) Hou, Z. R., Wang, J., He, P., Wang, J., Qin, B., Liu, X. H., Lin, L. L., and Feng, X. M. Highly Enantioselective Insertion of Carbenoids into N-H Bonds Catalyzed by Copper(I) Complexes of Binol Derivatives, *Angew. Chem. Int. Ed.* **2010**, *49*, 4763-4766.

(43) Li, M. L., Yu, J. H., Li, Y. H., Zhu, S. F., and Zhou, Q. L. Highly enantioselective carbene insertion into N-H bonds of aliphatic amines, *Science* **2019**, *366*, 990-994.

(44) Lee, E. C., and Fu, G. C. Copper-catalyzed asymmetric N-H insertion reactions: Couplings of diazo compounds with carbamates to generate alpha-amino acids, *J. Am. Chem. Soc.* **2007**, *129*, 12066-12067.

(45) Najera, C., and Sansano, J. M. Catalytic asymmetric synthesis of alpha-amino acids, *Chem. Rev.* **2007**, *107*, 4584-4671.

(46) Terstiege, I., Perry, M., Petersen, J., Tyrchan, C., Svensson, T., Lindmark, H., and Oster, L. Discovery of triazole aminopyrazines as a highly potent and selective series of PI3K delta inhibitors, *Bioorg. Med. Chem. Lett.* **2017**, *27*, 679-687.

(47) Frigerio, M., Hummersone, M. G., Menear, K. A., Finlay, M. R. V., Griffen, E. J., Ruston, L. L., Morris, J. J., Ting, A. K. T., Golding, B. T., Griffin, R. J., Hardcastle, I. R., and Rodriguez-Aristegui, S. (2010) WO patent 2010136778.

(48) Tinoco, A., Wei, Y., Bacik, J.-P., Carminati, D. M., Moore, E. J., Ando, N., Zhang, Y., and Fasan, R. Origin of High Stereocontrol in Olefin Cyclopropanation Catalyzed by an Engineered Carbene Transferase, *ACS Catal.* **2019**, *9* 1514-1524

(49) Wei, Y., Tinoco, A., Steck, V., Fasan, R., and Zhang, Y. Cyclopropanations via Heme Carbenes: Basic Mechanism and Effects of Carbene Substituent, Protein Axial Ligand, and Porphyrin Substitution, *J. Am. Chem. Soc.* **2018**, *140*, 1649-1662.

(50) Olson, J. S., Mathews, A. J., Rohlfs, R. J., Springer, B. A., Egeberg, K. D., Sligar, S. G., Tame, J., Renaud, J. P., and Nagai, K. The Role of the Distal Histidine in Myoglobin and Hemoglobin, *Nature* **1988**, *336*, 265-266.

(51) Moore, E. J., and Fasan, R. Effect of proximal ligand substitutions on the carbene and nitrene transferase activity of myoglobin, *Tetrahedron* **2019**, *75*, 2357-2363.

(52) Hayashi, Y., Aita, T., Toyota, H., Husimi, Y., Urabe, I., and Yomo, T. Experimental Rugged Fitness Landscape in Protein Sequence Space, *Plos One* **2006**, *1*.

(53) Kille, S., Zilly, F. E., Acevedo, J. P., and Reetz, M. T. Regio- and stereoselectivity of P450-catalysed hydroxylation of steroids controlled by laboratory evolution, *Nat. Chem.* **2011**, *3*, 738-743.

(54) Knight, A. M., Kan, S. B. J., Lewis, R. D., Brandenberg, O. F., Chen, K., and Arnold, F. H. Diverse Engineered Heme Proteins Enable Stereodivergent Cyclopropanation of Unactivated Alkenes, *ACS Central Sci.* **2018**, *4*, 372-377.

Graphical Abstract

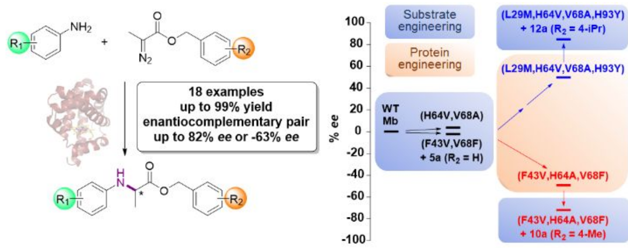

Synopsis

A first biocatalytic strategy for the asymmetric synthesis of chiral amines via carbene N—H insertion is reported.